Single-Electron Capacitance Spectroscopy of Few-Electron Artificial Atoms in a Magnetic Field: Theory and Experiment

Pawel Hawrylak

Institute for Microstructural Sciences, National Research Council of Canada, Ottawa, Canada K1A 0R6

(Received 20 May 1993)

The evolution of charging energies of few-electron artificial atoms (quantum dots) with magnetic field is calculated and compared with results of the single-electron capacitance spectroscopy of Ashoori *et al.* The evidence for magnetic field induced spin and angular momentum transitions in the strongly interacting artificial atom is presented.

PACS numbers: 73.20.Dx, 71.50.+t, 71.45.Gm

Artificially made atoms are quantum dots created in semiconductor heterostructures by laterally confining a two-dimensional electron gas [1]. In a typical vertical (or capacitor) structure the number of electrons can be well controlled and a small number N ($N=1,2,3,4\ldots$) of electrons per dot has been achieved experimentally [2,3]. The number of electrons is increased by changing the gate voltage and charging the dot with an additional *single* electron. The charging of a quantum dot with a single electron changes the capacitance of the structure. This method is called a single-electron capacitance spectroscopy (SECS) [3]. The charging of an N electron atom takes place when the chemical potential μ_E of the electrode equals the chemical potential $\mu_A(N)$ of the atom. The chemical potential $\mu_A(N)$ is equal to the energy required to add an extra electron $\mu_A(N)=E(N+1)-E(N)$ and thus SECS indirectly measures ground state energies $E(N)$. The ground state energy of an artificial atom is determined by a competition of kinetic, Zeeman, and electron-electron interaction energies leading to a series of incompressible states with "magic angular momentum" values [4]. The interaction of electrons in a strong magnetic field has been studied in the context of the incompressible liquid of the fractional quantum Hall effect [4–6] and is predicted to affect strongly transport [7], thermodynamic [8], and optical properties [9,10] of artificial atoms. In this work we demonstrate the importance of these effects on charging energies of few-electron artificial atoms in a magnetic field. Our calculations are compared with recent SECS results of Ashoori *et al.* [3] and the evidence for magnetic field induced spin and angular momentum transitions in the strongly interacting artificial atom is presented.

We start by emphasizing several important differences between real and artificial atoms. Some of these differences are associated with the semiconductor host material: the variable electron effective mass m and the screening of repulsive electron-electron interactions via the effective dielectric constant ε_0. As a consequence, artificial atoms in extremely high magnetic fields can be studied in laboratories. The most significant difference, however, is that in real atoms electrons move in a confining potential of the nucleus which is *singular*, while the confining potential of artificial atoms is *nonsingular*. While both potentials have identical geometrical symmetries associated with angular momenta, they differ in *hidden dynamical* symmetries and associated constants of motion. The Runge-Lenz vector is a well known additional constant of motion in the Coulomb problem. Since the nonsingular potential can always be approximated by a parabolic (harmonic) confining potential, the degrees of freedom in the artificial atom associated with center of mass motion separate from the relative motion of electrons [8,10]. Only the relative motion is affected by electron-electron interactions. This property makes artificial atoms similar to extended systems.

We outline here calculations of the electronic structure of artificial atoms based on Schwinger's coupled boson representation [10,11] which explicitly incorporates these two fundamental features: hidden symmetries and separability of the center of mass and relative motion. Explicit results for charging energies of few-electron atoms ($N=0,1,2,3$) are compared with experiment.

We consider a two-dimensional artificial atom (dot) containing N electrons confined by an externally imposed parabolic potential with a characteristic energy ω_0 and moving in the field of a fictitious nucleus (gate) with a positive charge $+Ne$ at a distance d away from the plane of the dot. The atom is placed in a magnetic field B normal to the plane of the dot. The positive charge assures charge neutrality of the atom and plays the role of the gate. For a dot size much smaller than d, we can approximate the *nonsingular* potential $V(r)$ of the positive charge by $-e^2N/\varepsilon_0 d+\frac{1}{2}(e^2N/\varepsilon_0 d^3)r^2$. Therefore the positive charge contributes a constant term and a parabolic term. The larger the number of carriers N, the stronger the single particle confinement. The Hamiltonian for N electrons can be written as

$$H=\sum_{i=1}^{N}\left[-\alpha N+\frac{1}{2m}\left(\mathbf{p}_i+\frac{e}{c}\mathbf{A}_i\right)^2+\frac{1}{2}m\omega_N^2\mathbf{r}_i^2+g\mu_B S_z^i B\right]+\sum_{i<j;i,j=1}^{N}\frac{e^2}{\varepsilon_0|\mathbf{r}_i-\mathbf{r}_j|}. \quad (1)$$

The vector potential is given in the symmetrical gauge, g is the effective g factor, μ_B is the Bohr magneton, S_z^i is the z component of the ith particle spin, and $\alpha=e^2/\varepsilon_0 d$. The effective confining frequency ω_N depends on the

0031-9007/93/71(20)/3347(4)$06.00

number of particles and is given by $\omega_N=[(\omega_0)^2+e^2N/m\varepsilon_0 d^3]^{1/2}$, and we take $\hbar=1$.

In order to introduce a coupled boson representation for the single particle Hamiltonian of the dot we introduce a pair of harmonic oscillator lowering (raising) operators (a,b) for each particle [10] $z^*=\sqrt{l_0^2/2\Omega}(a^\dagger+b)$, $z=\sqrt{l_0^2/2\Omega}(a+b^\dagger)$, $\partial_z=\sqrt{\Omega/2l_0^2}(b-a^\dagger)$, $\partial_z^*=\sqrt{\Omega/2l_0^2}(a-b^\dagger)$, where $z=(x-iy)/2$, $l_0=l/(m\omega_c)^{1/2}$ is the magnetic length, ω_c is the cyclotron energy, and $\Omega=[1+(2\omega_N/\omega_c)^2]^{1/2}$. The single particle Hamiltonian for an electron in the dot reduces to the Hamiltonian of a two-dimensional anisotropic harmonic oscillator with eigenenergies $E_{n,m}=\Omega_+(n+\frac{1}{2})+\Omega_-(m+\frac{1}{2})$, eigenstates $|m,n\rangle$ given by $|m,n\rangle=(b^\dagger)^m(a^\dagger)^n|0\rangle/(n!m!)^{1/2}$ and two different frequencies $\Omega_\pm=\{\sqrt{\omega_c^2+4\omega_N^2}\pm\omega_c\}/2$. The dynamical symmetries of the problem are now revealed by introducing the Schwinger angular momentum representation (11) $\mathbf{J}$, $\hat{j}$, $\mathbf{J}=(a^\dagger b^\dagger)\sigma/2(\hat{j})$, $\hat{j}=(a^\dagger b^\dagger)\times 1/2(\hat{j})$, where σ are Pauli matrices. The components of the operator $\mathbf{J}$ satisfy the usual commutation relations: $[J_i,J_j]=-i\varepsilon_{ijk}J_k$, and $\mathbf{J}^2=\hat{j}(\hat{j}+1)$. All conserved quantities are determined by the algebra of commuting operators. The eigenvalues of j and J_z are $0,\frac{1}{2},1,\frac{3}{2},\ldots$. The Hamiltonian can now be simply expressed in terms of operators j and J_z as $H=\Omega(\hat{j}+\frac{1}{2})-\omega_c\hat{J}_z$. Note that the breaking of continuous symmetry associated with the total 3D angular momentum in the original Hamiltonian due to the restriction of the motion of electrons to 2D results in a rather peculiar dependence of the Hamiltonian on j but not on J^2.

We now turn to the construction of many electron states which automatically separates the center of mass (c.m.) motion and the relative motion of electrons. This is accomplished through a unitary transformation $U(\phi)$ transforming individual particle boson creation operators $(a_i^\dagger)$ into c.m. and relative creation operators $(A_i^\dagger)$ [12]:

$$\begin{pmatrix} A_{\text{c.m.}}^\dagger \\ A_2^\dagger \\ A_3^\dagger \\ A_4^\dagger \\ \vdots \\ A_N^\dagger \end{pmatrix} = \frac{1}{\sqrt{N}} \begin{pmatrix} 1 & 1 & 1 & 1 & \cdots & 1 \\ e^{i\phi} & e^{i2\phi} & e^{i3\phi} & e^{i4\phi} & \cdots & e^{iN\phi} \\ e^{i2\phi} & e^{i4\phi} & e^{i6\phi} & e^{i8\phi} & \cdots & e^{i2N\phi} \\ e^{i3\phi} & e^{i6\phi} & e^{i9\phi} & e^{i12\phi} & \cdots & e^{i3N\phi} \\ \vdots & \vdots & \vdots & \vdots & \vdots & \vdots \\ e^{i(N-1)\phi} & \cdot & \cdot & \cdot & \cdot & \cdot \end{pmatrix} \begin{pmatrix} a_1^\dagger \\ a_2^\dagger \\ a_3^\dagger \\ a_4^\dagger \\ \vdots \\ a_N^\dagger \end{pmatrix}, \tag{2}$$

where $\phi=2\pi/N$. Operators $\{a_i\}$ transform according to $U(-\phi)$, and operators $\{b_i,b_i^\dagger\}$ transform into operators $\{B_i,B_i^\dagger\}$ identically to operators $\{a_ia_i^\dagger\}$. It is easy to see that the transformation U preserves boson commutation relations among operators (A,B) and that center of mass motion separates from the Hamiltonian. The motion of remaining $N-1$ relative particles is governed by the relative Hamiltonian (we drop the constant term αN)

$$H_{\text{rel}}=\sum_{i=2}^{N}\Omega_+(N_i+\tfrac{1}{2})+\Omega_-(M_i+\tfrac{1}{2})+\sum_{\mathbf{q}}\sum_{i<j}^{N}v(q)e^{-2|Q|^2}\{\exp[iQ^*(a_i^\dagger-a_j^\dagger)]\}\{\exp[iQ(a_i-a_j)]\}$$
$$\times\{\exp[iQ(b_i^\dagger-b_j^\dagger)]\}\{\exp[iQ^*(b_i-b_j)]\}, \tag{3}$$

where $Q=(q_x+q_y)l_0/\sqrt{2\Omega}$ and $v(q)=2\pi e^2/\varepsilon_0 q$. The relative Hamiltonian depends only on relative coordinates via $a_i^\dagger-a_j^\dagger=\sum_{l=2}^{N}(U_{il}^\dagger-U_{jl}^\dagger)A_l^\dagger$. The states of the relative Hamiltonian are built from simple products of single particle states $\prod_{i=2}^{N}|N_iM_i\rangle$ and spin states by the use of the antisymmetric operator $\hat{A}s=\sum_{i=1}^{N!}\mathrm{Det}(P_i)P_i$. Here P_i are elements of the $(N-1)$-dimensional representation of the permutation group S_N. This procedure, when applied to individual electron states, gives simple Slater determinants. The construction of the $N-1$ representations of the S_N is accomplished by a similarity transformation $U\hat{\mathbf{P}}U^\dagger$ applied to the standard N-dimensional representation of S_N, and dropping the first row and first column ($\hat{\mathbf{P}}$ is the regular N-dimensional representation).

Note that the transformation U also transforms the N electron spin wave function $\chi(S_z)$ for $S_z=(N-1)/2$ (a single reversed spin) into spin states $\chi(S,S_z)$ characterized not only by the total spin projection S_z but also total spin S. There is a clear analogy between projecting out the c.m. degrees of freedom and looking at spin reversed excitations.

This general procedure is best illustrated for the first nontrivial case of three electrons [9] ($N=3$). There are two pairs of relative operators $\{A_2^\dagger,A_3^\dagger\}$, $\{B_2^\dagger,B_3^\dagger\}$ and six elements of the permutation group $\{P_i\}$:

$$\left\{\begin{pmatrix}1&0\\0&1\end{pmatrix};\begin{pmatrix}e^{+i\varphi}&0\\0&e^{-i\varphi}\end{pmatrix};\begin{pmatrix}e^{-i\varphi}&0\\0&e^{+i\varphi}\end{pmatrix};\begin{pmatrix}0&1\\1&0\end{pmatrix};\begin{pmatrix}0&e^{+i\varphi}\\e^{-i\varphi}&0\end{pmatrix};\begin{pmatrix}0&e^{-i\varphi}\\e^{+i\varphi}&0\end{pmatrix}\right\}.$$

The three-electron states are classified by a total spin S and its projection S_z. There is one quartet

$$\{\chi(S,S_z)=\chi(\tfrac{3}{2},+\tfrac{3}{2}),\chi(\tfrac{3}{2},+\tfrac{1}{2}),\chi(\tfrac{3}{2},-\tfrac{1}{2}),\chi(\tfrac{3}{2},-\tfrac{3}{2})\}$$

and a pair of doublets

$$\{\chi(S,S_z)=\{\chi_2(\tfrac{1}{2},+\tfrac{1}{2}),\chi_3(\tfrac{1}{2},+\tfrac{1}{2})\};\{\chi_2(\tfrac{1}{2},-\tfrac{1}{2}),\chi_3(\tfrac{1}{2},-\tfrac{1}{2})\}\}.$$

The antisymmetric states are generated from a product of spin $\{\chi(S,S_z)\}$ and harmonic oscillator states $|N_2,N_3,M_2,M_3\rangle$ using the antisymmetrization operator As. This is readily accomplished because operations P_i merely

correspond to simply adding a phase and/or interchanging relative operators. For example, for the spin polarized system ($S=\frac{3}{2}, S_z=-\frac{3}{2}$) the correlated basis $|N_2,N_3,M_2,M_3\rangle^{as}$ (Laughlin states) of a quantum dot turns out to be a simple combination of harmonic oscillator states:

$$|N_2,N_3,M_2,M_3\rangle^{as}=\frac{1+2\cos[2\pi(N_2-N_3+M_2-M_3)/3]}{3\sqrt{2}}(|N_2,N_3,M_2,M_3\rangle-|N_3,N_2,M_3,M_2\rangle).$$

These states exist only if the quantum number $L=M_2-M_3+N_2-N_3=3m$, with $m=1,2,3\ldots$. Hence statistics introduces additional symmetries which result in restricted coupled boson states. Similar results can be derived for spin doublets ($S=\frac{1}{2}$) for which quantum number L is restricted to $L=3m+1$, but with $m=\ldots-2,-1,0,+1,+2\ldots$. Examining the form of the relative Hamiltonian we find another conserved quantity: the total relative angular momentum $R=(M_2+M_3)-(N_2+N_3)$. The energy spectrum of the *relative* Hamiltonian is now diagonalized for each value of the relative angular momentum R using correlated states drawn from up to four Landau levels as a basis [13]. We take the bare confining potential to be $\omega_0=3.31$ meV, the distance d of the nucleus to the plane of the dot $d=1000$ Å, $\alpha=1.2$ meV, and other parameters, e.g., effective mass and dielectric constant, appropriate for GaAs. The Zeeman splitting is taken to be $\Delta E_z=g\mu B$, which for GaAs (g factor of 0.52) gives $\Delta E_z=0.03$ meV/T. All energy spectra are plotted with respect to the vacuum energy $E_v=N(\Omega_+ + \Omega_-)/2$ which includes the zero point motion of the center of mass. The calculated ground state energies for $N=2$ and $N=3$ are shown in Figs. 1(a) and 1(b), and are labeled by a total spin S and relative angular momentum R. The cusps in the ground state energy as a function of the magnetic field are due to the change in the spin polarization and changes of the ground state angular momentum of the relative motion both for the two- and three-electron atoms. The change of the angular momentum with the magnetic field can be easily understood in terms of the competition between kinetic energy, Zeeman energy, and repulsive electron-electron interaction energy. The contribution from kinetic energy decreases as it is proportional to Ω_- while the contribution from *e-e* interaction (proportional to $B^{1/2}$) and Zeeman energy (proportional to B) increases. At low B electrons minimize their kinetic energy by occupying a small area of the dot, while as the magnetic field increases electrons maintain a larger area minimizing mutual repulsion. The area is quantized due to restrictions on possible quantum numbers R and L leading to incompressible spin-polarized states with restricted values of relative angular momentum $R=3,6,9,12,\ldots$.

In Fig. 1(c) we show the magnetic field dependence of the charging energy [without the kinetic energy $E(1)$] $\mu_A(2)-E(1)=E(3)-E(2)-E(1)$ of a two-electron dot. The charging energy exhibits a number of structures: the peak around $B=2$ T (A) corresponds to a spin singlet-spin triplet transition in a two-electron atom, followed by a spin-unpolarized ($S=\frac{1}{2}$ doublet) to spin-polarized ($S=\frac{3}{2}$ quartet) transition in the three-electron atom. The peak around $B=5$ T (B) corresponds to transitions back to spin-unpolarized–spin-polarized states and change in the angular momentum of the three-electron atom from $R=3$ to $R=6$. The structure (dip) around $B=6$ T (C) corresponds to the spin and angular momentum change in the two-electron atom. Small oscillations at higher magnetic fields correspond to transitions between different incompressible spin-polarized states of the three-electron atom, with a dip at around $B=13$ T corresponding to a change in the angular momentum state of the spin triplet state of the two-electron atom.

The SECS technique and basic configuration of the sample has been described recently by Ashoori *et al.* [3]. The SECS measures charging energies of a vertical quantum dot based on a 175 Å quantum well with lateral confinement provided by a metallic gate. We concentrate on a small number of electrons because for up to four electrons there is *no* structure in the charging energy of *noninteracting* electrons. All changes are driven by Coulomb interactions. In Fig. 2 we show the experimental results [3] (solid circles) and calculated (solid line) dependence of the charging energy of a two-electron

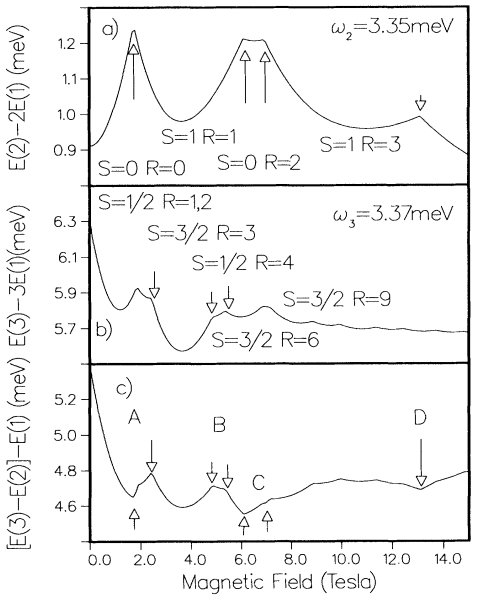

FIG. 1. (a) Ground state energy of a two-electron artificial atom as a function of the magnetic field, (b) ground state energy of a three-electron artificial atom as a function of the magnetic field, and (c) charging energy of a two-electron atom (no kinetic energy). Symbols indicate spin and angular momentum states of the ground state.

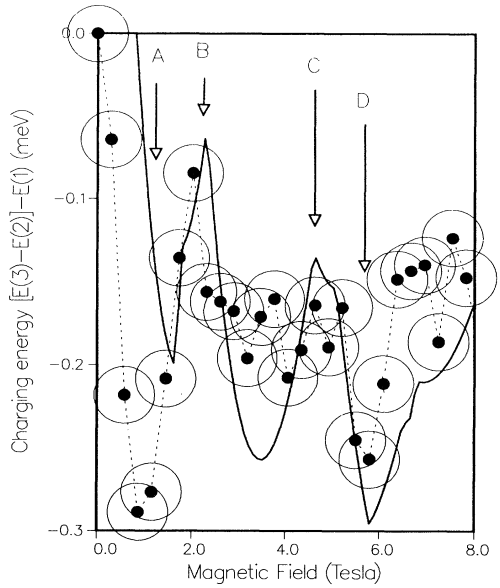

FIG. 2. Measured (solid circles) and calculated (solid line) charging energy, i.e., energy to add a third electron to the two-electron atom $\{[E(3)-E(2)]-E(1)\}$ as a function of the magnetic field (the vacuum energy subtracted from both curves). Letters A,B,C,D correspond to spin and angular momentum transitions in the two- and three-electron atoms. The size of the circle reflects experimental error of approximately 0.03 meV.

atom on the magnetic field. We have subtracted the kinetic energy contribution from the experimental charging energy, and shifted vertically the experimental versus calculated curves. The experimental error of approximately 0.03 meV is reflected in the size of experimental points [14]. There are four main structures in the experimental and calculated curves. We associate the first minimum below $B=2$ T (A) with spin singlet ($S=0,R=0$) and spin triplet ($S=1,R=2$) transitions in the two-electron atom. The following peak above $B=2$ T (B) is associated with the spin-unpolarized ($S=\frac{1}{2},R=2$) and spin polarized ($S=\frac{3}{2},R=3$) transition in the three-electron dot. The plateau between $B=2$ T and $B=5$ T corresponds to the incompressible state ($S=\frac{3}{2},R=3$) of the three-electron dot. The third peak (C) is associated primarily with the angular momentum transition in the three-electron atom between magic states $R=3$ and $R=6$. This transition is intertwined with the spin-polarized–spin-unpolarized transition [see Fig. 1(b)]. The fourth structure around $B=6$ T (D) corresponds to the suppression of charging energies mostly due to the angular momentum transition $R=1\rightarrow R=3$ in the two-electron atom. This transition is intertwined with the spin-polarized–spin-unpolarized transition [see Fig. 1(a)]. The calculated charging energies reflect reasonably well the position, magnitude, and shape of the experimental data. In particular, the energy scale of structures A, B, and D is well above experimental error. The visible discrepancies between experiment and theory could be due to the parameters of the experimental system: finite well width, presence of the gate and nonparabolic corrections to the potential, band nonparabolicity, and the presence of remote impurities. We have no reason to believe that these effects will introduce a crossing of lowest single particle energy levels and hence give rise to magnetic field induced structures in charging energies of few-electron dots. The very presence of oscillations in experimentally observed charging energies is clearly due to electron-electron interactions. To account for the magnitude of oscillations both improved calculations and better experiments are needed.

We studied the effect of spin, confinement, and electron-electron interactions on the dependence of charging energies of few-electron artificial atoms (quantum dots) with the magnetic field. Calculations including two important features of artificial atoms, dynamical symmetries and separability of the center of mass motion, were compared with results of the single-electron capacitance spectroscopy of Ashoori *et al.* The evidence for magnetic field induced spin and angular momentum transitions in the strongly interacting artificial atom is presented.

We thank R. Ashoori, H. L. Stormer, G. C. Aers, and C. Dharmawardana for discussions and R. Ashoori for providing his experimental data prior to publication.

[1] For a recent review and references, see T. Chakraborty, Comments Condens. Matter Phys. **16**, 35 (1992).
[2] Ch. Sikorski and U. Merkt, Phys. Rev. Lett. **62**, 2164 (1989); B. Meurer, D. Heitman, and K. Ploog, Phys. Rev. Lett. **68**, 1371 (1992); Bo Su, V. J. Goldman, and J. E. Cunningham, Science **255**, 313 (1992).
[3] R. C. Ashoori, H. L. Stormer, J. S. Weiner, L. N. Pfeiffer, K. W. Baldwin, and K. W. West, Phys. Rev. Lett. **71**, 613 (1993); **68**, 3088 (1992).
[4] R. B. Laughlin, Phys. Rev. B **27**, 3383 (1983).
[5] S. M. Girvin and Terrence Jach, Phys. Rev. B **28**, 4506 (1983).
[6] Yu. A. Bychkov, S. V. Iordanskii, and G. M. Eliashberg, Pis'ma Zh. Eksp. Teor. Fiz. **33**, 152 (1981) [JETP Lett. **33**, 143 (1981)]; Yu. Bychkov and E. I. Rashba, Zh. Eksp. Teor. Fiz. **96**, 757 (1989) [Sov. Phys. JETP **69**, 430 (1989)].
[7] P. L. McEuen, E. B. Foxman, Jari Kinaret, U. Meirav, M. A. Kastner, N. S. Wingreen, and S. J. Wind, Phys. Rev. B **45**, 11419 (1992); A. S. Sachrajda, R. P. Taylor, C. Dharma-Wardana, P. Zawadzki, J. A. Adams, and P. T. Coleridge, Phys. Rev. B **47**, 6811 (1993).
[8] P. A. Maksym and Tapash Chakraborty, Phys. Rev. Lett. **65**, 108 (1990); Phys. Rev. B **45**, 1947 (1992).
[9] D. Pfannkuche and R. R. Gerhardts, Phys. Rev. B **44**, 13132 (1991).
[10] P. Hawrylak and D. Pfannkuche, Phys. Rev. Lett. **70**, 485 (1993).
[11] D. C. Mattis, *The Theory of Magnetism* (Springer-Verlag, Berlin, 1988).
[12] P. Maksym, Physica (Amsterdam) **184B**, 385 (1993).
[13] P. Hawrylak (to be published).
[14] R. Ashoori (private communication).